# Two-Dimensional Harmonic Balance Finite Element Modelling of Electrical Machines taking Motion into account

J. Gyselinck[1], L. Vandevelde[2], A. M. Oliveira[3], P. Dular[1], J. Melkebeek[2], and P. Kuo-Peng[3]

[1]Institut Montefiore, Department of Electrical Engineering, University of Liège
Sart Tilman B28, B-4000 Liège, Belgium
phone: +32 4 366 37 32 – fax: +32 4 366 29 10 – e-mail: Johan.Gyselinck@ulg.ac.be

[2]Laboratory for Electrical Power Engineering
Department of Electrical Energy, Systems and Automation, Ghent University
Sint-Pietersnieuwstraat 41, B-9000 Ghent, Belgium

[3]Design and Analysis of Electromagnetic Devices Group (GRUCAD)
Electrical Engineering Department, Federal University of Santa Catarina
88040–900 Floripanópolis, SC 476, Brazil

***Abstract* – An original and easy-to-implement method to take into account movement in the 2D harmonic balance finite element modelling of electrical machines is presented. The global harmonic balance system of algebraic equations is derived by applying the Galerkin approach to both the space and time discretisation. The harmonic basis functions, i.e. a cosine and a sine function for each nonzero frequency and a constant function 1 for the dc component, are used for approximating the periodic time variation as well as for weighing the time domain equations in the fundamental period. In practice, this requires some elementary manipulations of the moving band stiffness matrix. Magnetic saturation and electrical circuit coupling are easily included in the analysis.**

**As an application example, the noload operation of a permanent magnet machine is considered. The voltage and induction waveforms obtained with the proposed harmonic balance method are shown to converge well to those obtained with time stepping.**

## 1. Introduction

The steady-state finite element (FE) analysis of electrical machines can be carried out either in the time domain or the frequency domain. The first approach, also referred to as time stepping, is mostly followed, in spite of the very large number of time steps to be carried out. Indeed, the time step $\Delta t$ to be adopted, which depends on the largest relevant frequency of the system under study, may be very small and in some cases the transient phenomenon that has to be stepped through before reaching quasi steady-state may decay very slowly.

The frequency domain or harmonic balance (HB) approach [1],[2] is not very popular as it has some evident disadvantages. It consists in approximating the periodic time variation of the magnetic fields by a truncated Fourier series and results in a single but very large system of nonlinear algebraic equations. Its resolution may be very expensive as both the number of unknowns and the bandwidth increase with the number of considered frequencies.

Furthermore, it is difficult to take saturation and movement into account. Some of the authors have treated the first aspect, the magnetic nonlinearity, in a recent publication [3]. The nonlinear HB equations are straightforwardly solved by means of the Newton-Raphson method. In this paper, the authors focus on the motional aspect, and extend the method proposed in [3] to problems with periodic movement. In particular, a 2D FE model of a rotating electrical machine having a moving band is considered. The approach can be equally adopted for an arbitrary time periodic movement (in e.g. linear machines) if a hybrid finite element – boundary element model is used [4].

It should be noted that sofar the modelling of electrical machines in the frequency domain has been awarded little attention in the literature, unlike its time domain counterpart. However, one particular case of frequency domain calculations has been and still is extensily carried out. It concerns the harmonic simulation of static devices and induction machines [5], in which only one frequency is considered. In induction machines, the slip frequency in the rotor is simply effected by multiplying the conductivity of the rotor bars by the slip. The saturation is taken into account by means of an equivalent $bh$-curve, the choice of which may affect considerably the accuracy [6]. Obviously the single-frequency approach can only produce a (rough) estimate of the fundamental components. A more involved approach consists in e.g. considering a multi-harmonic stator and rotor model separately and identifying the airgap fields of corresponding time and spatial order [7].

In the following sections, the extension of the HBFE method to rotating electrical machines will be elaborated and applied to a permanent-magnet machine.

## 2. Outline of the method

### *A. 2D magnetostatic problem*

We consider a classical 2D magnetostatic problem [8]. In a domain $\Omega$ in the $xy$-plane, the given current density $\underline{j} = j(x,y)\,\underline{1}_z$ is directed along the $z$-axis. The magnetic field $\underline{h}$ and the magnetic induction $\underline{b}$, the $z$-component of which vanishes, are to be calculated. The constitutive law $\underline{h} = \nu\,\underline{b}$, with $\nu$ the reluctivity, and conditions on the boundary of $\Omega$ are supplied.

Permanent magnets can be included in the analysis as well. The constitutive law $\underline{h} = \nu\,(\underline{b} + \underline{b}_r)$, where $\underline{b}_r$ is the remanent induction, leads to an equivalent current density $-\mathrm{curl}\,(\nu\,\underline{b}_r)$ in the permanent-magnet domains and to a current layer on their boundary. In case of a uniform magnetisation (constant $\nu\underline{b}_r$), only the latter is nonzero.

The magnetostatic field problem is mostly formulated in terms of the magnetic vector potential $\underline{a}(x,y)$, which can be chosen along the $z$-axis: $\underline{a} = a(x,y)\,\underline{1}_z$. From $\underline{b} =$

$\operatorname{curl} \underline{a} = \underline{1}_z \times \operatorname{grad} a$, it follows that the magnetic Gauss law $\operatorname{div} \underline{b} = 0$ automatically holds. Remains to satisfy Ampère's law $\operatorname{curl} \underline{h} = \underline{j}$, which, expressed in terms of the magnetic vector potential, reads:

$$\operatorname{curl} (\nu \operatorname{curl} \underline{a}) = \underline{j} \quad \text{or} \quad \operatorname{div} (\nu \operatorname{grad} a) = -j \,. \tag{1}$$

A discretisation of the domain $\Omega$ in e.g. first order triangular elements allows to approximate the potential $a(x, y)$ as

$$a(x, y) = \sum\nolimits_{l=1}^{\#n} a_l \, \alpha_l(x, y), \tag{2}$$

where $\alpha_l(x, y)$ is the piecewisely linear basis function that is associated with the $l$-th node in the FE mesh. The total number of nodes is denoted $\#n$.

Following the Galerkin approach, (1) is weakly imposed in $\Omega$ by weighing it with all $\#n$ interpolation functions $\alpha_k(x, y)$:

$$\int_\Omega \Big( \operatorname{div}(\nu \operatorname{grad} a) + j \Big) \, \alpha_k \, \mathrm{d}\Omega \;=\; 0 \,. \tag{3}$$

Considering (2), partial integration of (3) produces a system of $\#n$ algebraic equations in terms of the $\#n$ unknown coefficients $a_l$. If the problem is linear (considering a constant reluctivity $\nu$), the system of equations is linear as well. It can be written as follows:

$$\boldsymbol{S} \boldsymbol{A} = \boldsymbol{J}, \tag{4}$$

where $\boldsymbol{A}$ is the column matrix in which the $\#n$ unknowns are assembled, and where the elements of the square stiffness matrix $\boldsymbol{S}$ and the column matrix $\boldsymbol{J}$ are given by

$$S_{kl} \;=\; \int_\Omega \nu \operatorname{grad} \alpha_k \cdot \operatorname{grad} \alpha_l \, \mathrm{d}\Omega \,, \tag{5}$$

$$J_k \;=\; \int_\Omega j(x, y) \, \alpha_k \, \mathrm{d}\Omega \,. \tag{6}$$

For the sake of brevity, the boundary conditions and permanent magnets are not explicitly considered in the present analysis.

### *B. Rotating electrical machines*

For modelling rotating electrical machines, the FE domain $\Omega$ is commonly split up into three complementary subdomains: a "stator" $\Omega_s$, a "rotor" $\Omega_r$ and a thin ring $\Omega_{mb}$ between stator and rotor, the so-called moving band (see Fig. 1).

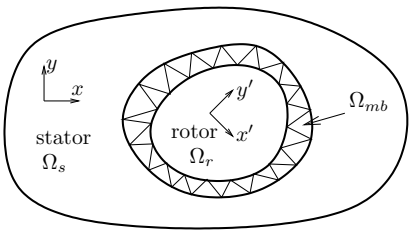


Fig. 1. 2D FE model consisting of a stator $\Omega_s$, a rotor $\Omega_r$ and a moving band $\Omega_{mb}$

As the rotor angle $\theta$ varies in time, the FE mesh in the stator and the rotor can remain identical with regard to the respective reference frames $xy$ and $x'y'$, while the moving band needs to be remeshed. For sake of convenience, the stator and the rotor are connected by a single layer of elements in the moving band. As the rotor position changes, the discretisation of the moving band changes in a discontinuous way: the elements are deformed and, intermittently, the topology of the moving band mesh is (locally) modified in order to maintain elements of good aspect ratio.

As there are no nodes situated inside the moving band, the total number of nodes $\#n$ does not vary with the rotor angle $\theta(t)$, and equals $\#n_s + \#n_r$, the number of nodes in the stator and the rotor respectively.

When written in terms of the proper coordinates (i.e. in the stator or the rotor reference frame), the interpolation functions are $\theta$-independent, and the interpolation of the magnetic vector potential can be expressed as

$$a(x, y, t) \;=\; \sum\nolimits_{l=1}^{\#n_s} a_{sl}(t) \, \alpha_{sl}(x, y) \quad \text{in} \quad \Omega_s \,, \tag{7}$$

$$a(x', y', t) \;=\; \sum\nolimits_{l=1}^{\#n_r} a_{rl}(t) \, \alpha_{rl}(x', y') \quad \text{in} \quad \Omega_r \,. \tag{8}$$

In the moving band $\Omega_{mb}$, the interpolation is inherently $\theta$-dependent:

$$a = \sum_{sl} a_{sl}(t) \, \alpha_{sl}(x, y, \theta) + \sum_{rl} a_{rl}(t) \, \alpha_{rl}(x', y', \theta) \,, \tag{9}$$

where only the basis functions $\alpha_{sl}$ and $\alpha_{rl}$ associated with nodes on the outer and the inner boundary respectively of the moving band are to be considered.

The system of algebraic equations (4) can be partitioned accordingly:

$$\begin{bmatrix} \boldsymbol{S}^s_{ss} + \boldsymbol{S}^{mb}_{ss} & \boldsymbol{S}^{mb}_{sr} \\ \boldsymbol{S}^{mb}_{rs} & \boldsymbol{S}^r_{rr} + \boldsymbol{S}^{mb}_{rr} \end{bmatrix} \begin{bmatrix} \boldsymbol{A}_s \\ \boldsymbol{A}_r \end{bmatrix} = \begin{bmatrix} \boldsymbol{J}_s \\ \boldsymbol{J}_r \end{bmatrix}, \tag{10}$$

where the subscripts indicate the concerned degrees of freedom and the superscript ($s$, $r$ or $mb$) indicates the subdomain that produces the block in the stiffness matrix.

When ignoring saturation, the diagonal blocks $\boldsymbol{S}^s_{ss}$ and $\boldsymbol{S}^r_{rr}$, due to the stator and the rotor respectively, are time-invariant. The blocks $\boldsymbol{S}^{bm}_{ss}$, $\boldsymbol{S}^{bm}_{rr}$ and $\boldsymbol{S}^{bm}_{sr} = (\boldsymbol{S}^{bm}_{rs})^T$, due to the moving band, depend on the rotor position $\theta(t)$.

### *C. Harmonic balance*

Let us now consider a time periodic problem. The current and/or permanent magnet excitation, $\boldsymbol{J}_s(t)$ and $\boldsymbol{J}_r(t)$, and the rotor position $\theta(t)$ (modulo $2\pi$) vary periodically in time, with fundamental frequency $f$ and period $T = 1/f$.

The harmonic balance method consists in approximating the periodic time variation of $\boldsymbol{A}_s(t)$ and $\boldsymbol{A}_r(t)$ by a truncated Fourier series. The corresponding time basis functions $H(t)$ are $\sqrt{2}\cos(2\pi k f t)$ and $-\sqrt{2}\sin(2\pi k f t)$ for each nonzero frequency $kf$, and a constant function 1 for the dc component. A different set of frequencies may be adopted in the stator and the rotor.

The harmonic time discretisation of $\boldsymbol{A}_s(t)$ and $\boldsymbol{A}_r(t)$ can thus be written as

$$\boldsymbol{A}_s(t) \;=\; \sum\nolimits_{\lambda=1}^{\#h_s} \boldsymbol{A}^{(\lambda)}_s H_{s\lambda}(t) \,, \tag{11}$$

$$\boldsymbol{A}_r(t) \;=\; \sum\nolimits_{\lambda=1}^{\#h_r} \boldsymbol{A}^{(\lambda)}_r H_{r\lambda}(t) \,, \tag{12}$$

where $\#h_s$ is the number of harmonic basis functions considered in the stator and the moving band, and where $\#h_r$ is the number of functions in the rotor and the moving band. In the moving band, both sets of frequencies apply.

The harmonic basis functions are orthonormal in the stator and the rotor respectively. E.g., for those defined in the

stator:

$$\frac{1}{T}\int_0^T H_{s\kappa}(t)\, H_{s\lambda}(t)\,\mathrm{d}t = \delta_{\kappa,\lambda}\,. \tag{13}$$

Adopting the Galerkin approach, the HB system of algebraic equations can be obtained by using the harmonic basis function as test function as well. The weighing of (4) in the fundamental period $[0,T]$ with a basis function $H(t)$ can be written as

$$\frac{1}{T}\int_0^T \Big(\boldsymbol{S}\boldsymbol{A}-\boldsymbol{J}\Big)H(t)\,\mathrm{d}t \;=\; 0\,. \tag{14}$$

Considering the partitioned system (10) and the harmonic functions that are defined in the stator and the moving band on the one hand, and in the rotor and the moving band on the other hand, (14) can be further detailed to

$$\frac{1}{T}\int_0^T \Big((\boldsymbol{S}^s_{ss}+\boldsymbol{S}^{mb}_{ss})\boldsymbol{A}_s+\boldsymbol{S}^{mb}_{sr}\boldsymbol{A}_r-\boldsymbol{J}_s\Big)H_{s\kappa}\,\mathrm{d}t \;=\; 0\,, \tag{15}$$

$$\frac{1}{T}\int_0^T \Big(\boldsymbol{S}^{mb}_{sr}\boldsymbol{A}_s+(\boldsymbol{S}^r_{rr}+\boldsymbol{S}^{mb}_{rr})\boldsymbol{A}_r-\boldsymbol{J}_r\Big)H_{r\kappa}\,\mathrm{d}t \;=\; 0\,. \tag{16}$$

The time discretisation (11-12) thus leads to a system of $\#n_s\#h_s+\#n_r\#h_r$ linear equations in term of an equal number or unknowns. It can be written as follows:

$$\begin{bmatrix} \boldsymbol{S}^s_{ssH}+\boldsymbol{S}^{mb}_{ssH} & \boldsymbol{S}^{mb}_{srH} \\ \boldsymbol{S}^{mb}_{rsH} & \boldsymbol{S}^r_{rrH}+\boldsymbol{S}^{mb}_{rrH} \end{bmatrix}\begin{bmatrix}\boldsymbol{A}_{sH}\\ \boldsymbol{A}_{rH}\end{bmatrix}=\begin{bmatrix}\boldsymbol{J}_{sH}\\ \boldsymbol{J}_{rH}\end{bmatrix}, \tag{17}$$

The harmonic components of $\boldsymbol{A}_s(t)$ and $\boldsymbol{A}_r(t)$ are assembled in $\boldsymbol{A}_{sH}$ and $\boldsymbol{A}_{rH}$ as follows:

$$\boldsymbol{A}_{sH}=\begin{bmatrix}\boldsymbol{A}^{(1)}_s\\ \vdots\\ \boldsymbol{A}^{(\#h_s)}_s\end{bmatrix}\quad\text{and}\quad \boldsymbol{A}_{rH}=\begin{bmatrix}\boldsymbol{A}^{(1)}_r\\ \vdots\\ \boldsymbol{A}^{(\#h_r)}_r\end{bmatrix}, \tag{18}$$

and the matrices $\boldsymbol{S}^s_{ssH}$ etc. can be partitioned into blocks $\boldsymbol{S}^{s(\kappa,\lambda)}_{ssH}$ etc., where $(\kappa,\lambda)$ refers to the pair of harmonic functions concerned, i.e. $H_{s\kappa}(t)H_{s\lambda}(t)$, $H_{r\kappa}(t)H_{r\lambda}(t)$ or $H_{r\kappa}(t)H_{s\lambda}(t)$.

From the orthonormality of the basis functions (13), it follows that the matrices $\boldsymbol{S}^s_{ssH}$ and $\boldsymbol{S}^r_{rrH}$ have a diagonal block structure. Indeed, the blocks of e.g. $\boldsymbol{S}^s_{ssH}$ are given by

$$\boldsymbol{S}^{s(\kappa,\lambda)}_{ssH} \;=\; \frac{1}{T}\int_0^T \boldsymbol{S}^s_{ss}\, H_{s\kappa}(t)H_{s\lambda}(t)\,\mathrm{d}t \;=\; \delta_{\kappa,\lambda}\boldsymbol{S}_{ss}\,. \tag{19}$$

The matrices produced by the moving band generally have a full block structure. E.g., the blocks of $\boldsymbol{S}^{mb}_{srH}$ are given by

$$\boldsymbol{S}^{mb(\kappa,\lambda)}_{srH}=\frac{1}{T}\int_0^T \boldsymbol{S}^{mb}_{sr}(\theta(t))\, H_{s\kappa}(t)H_{r\lambda}(t)\,\mathrm{d}t\,. \tag{20}$$

Different harmonics in the stator (having the same or different frequency) are thus coupled through the nodes situated on the outer moving band contour. The same holds for the rotor harmonics and the nodes on the inner moving band contour. The stator and the rotor harmonics are coupled through all the nodes situated on outer and inner contour of the moving band.

### *D. Practical aspects and extension to nonlinear problems*

In practice, the integrals (20) over the fundamental period $[0,T]$ are approximated by a sum, considering a finite number of discrete time instants $t_i$. For each corresponding rotor position $\theta(t_i)$, the moving band is meshed and it static stiffness matrix is calculated. Then the contribution to the global HB system matrix is effected, considering all the relevant pairs of harmonic basis functions.

Saturation can be taken into account as proposed in [3]. The system of nonlinear algebraic equations can be solved straightforwardly by means of the Newton-Raphson (NR) method. Hereto, for each NR iteration and for each element situated in a nonlinear region of the FE domain, the differential reluctivity tensor $\frac{\partial \underline{\underline{h}}}{\partial \underline{b}}$ multiplied by each relevant pair of harmonic basis functions needs to be integrated over $[0,T]$. Saturation causes all harmonics considered in the nonlinear region to be coupled.

The constant contribution of the moving band (where the reluctivity is constant, $\nu=\nu_0$) and of the linear media in the stator and the rotor to the Jacobian matrices can be calculated and stored before starting the iterative NR process.

Electrical circuit coupling can be easily considered [9][2]. If the electrical circuit is linear, the electrical coupling does not require a special harmonic balance treatment. However, for nonlinear inductive components and resistive components (e.g. diodes), the differential inductance (flux derived with respect to current) and the differential resistance (voltage drop derived with respect to current) have to be processed in a similar way as the differential reluctivity tensor [10].

Both the time domain as the HB systems of algebraic equation can be solved by means of GMRES with ILU preconditioning, after renumbering with the reverse Cuthill McKee algorithm [11][12]. As the fill-in (average number of nonzero entries per row) increases with the number of considered frequencies, it is important for the GMRES convergence and the computational cost (computation time and storage requirements) to set the fill-in of the preconditioning to a appropriate value.

## 3. Application example

### *A. 2D FE model of permanent magnet machine*

The proposed HB method is applied to an eight-pole three-phase permanent-magnet motor [13]. The stator windings are star connected. The commercial motor has 24 *skewed* stator slots (one slot per pole and per phase) and the permanent magnets are mounted in a slightly asymmetric way. As a result, the distortion of the induced voltages is considerably reduced.

In this paper we consider an especially assembled motor, that has *straight* stator slots and in which the magnets are mounted (nearly) symmetrically. In the following, the measured noload voltage waveform will be compared to the one obtained with the 2D FE model using both the time and the frequency domain approach. Induction waveforms in stator and rotor will be shown as well.

By imposing anti-periodicity conditions, only one pole needs to be modelled. The FE discretisation is depicted in Fig. 2. The airgap is split up in three layers (see zoom in Fig. 2), the middle of which is the moving band. The mean

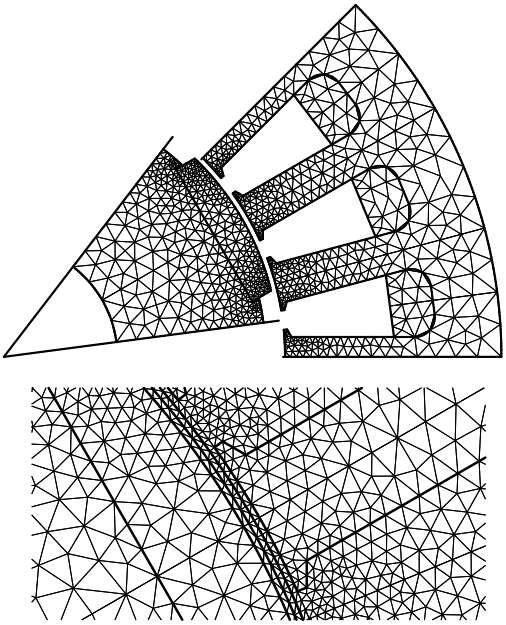

Fig. 2. 2D FE model of one pole of the permanent-magnet machine ($\#n = 1450$; 1880 first order triangles: 1880 in stator, 924 in rotor and 130 in moving band)

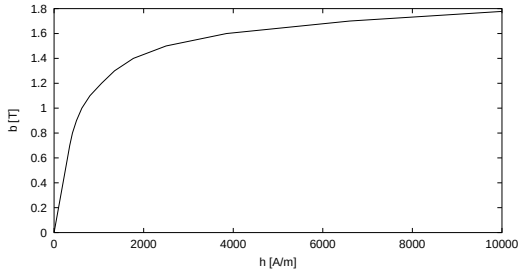


Fig. 3. $bh$-curve of stator and rotor iron

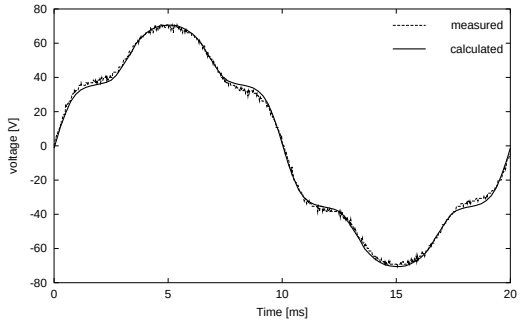


Fig. 4. Measured and calculated noload line-to-line voltage

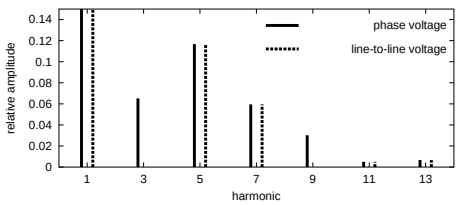


Fig. 5. Spectrum of line-to-line voltage and phase voltage (the amplitude of the fundamental 50 Hz component of the phase and line-to-line voltage is 38.5 V and 66.6 V respectively)

airgap radius and the minimum airgap width are 25.7 mm and 0.55 mm respectively. The axial length of the stator and the rotor core stack is 40 mm. The $bh$-curve used for the stator and the rotor iron is shown in Fig. 3.

### *B. Time-stepping simulation*

A time-stepping simulation at 750 rpm is carried out ($f = 50$ Hz, $T = 20$ ms). As it concerns a static problem with a constant excitation, there is no transient. One period is time-stepped with $\Delta t = T/360$.

In Fig. 4, the obtained line-to-line voltage waveform is shown together with the measured one. A good agreement is observed. The spectrum of the calculated line-to-line voltage and phase voltage is shown in Fig. 5. The phase voltage contains important 3rd, 5th, 7th and 9th harmonics. The $3k$ harmonics do not appear in the line-to-line voltage.

### *C. Harmonic balance simulations*

Besides the fundamental $f = 50$ Hz component in the stator and the dc component in the rotor, the magnetic field has odd harmonics $(2k + 1)f$ in the stator and $6f$ harmonics in the rotor.

Five HB calculations with increasing spectrum are carried out. They are denoted HB 1, HB 5, HB 7, HB 11 and HB 13, and comprise the following harmonics:

HB 1 : 0, 1
HB 5 : 0, 1, 3, 5
HB 7 : 0, 1, 3, 5, 6, 7
HB 11 : 0, 1, 3, 5, 6, 7, 9, 11
HB 13 : 0, 1, 3, 5, 6, 7, 9, 11, 12, 13

In HB 13, e.g., six nonzero frequencies are considered in the stator, while in the rotor, the dc component and two nonzero frequencies are considered. This results in a total of $12+5 = 17$ harmonic basis functions. For evaluating the HB stiffness matrix of the moving band numerically, 360 time instants in $[0, T]$ and rotor positions $\theta$ in $[0°, 90°]$ are considered.

Some of the obtained harmonic components of the flux pattern are shown in Fig. 6.

The waveform of the phase voltage obtained with the five HB calculations and with the time stepping simulation are depicted in Fig. 7. A good convergence of the HB waveforms to the time stepping one is observed. Note also that the distortion of the moving band elements may cause some noise in the calculation voltage, as can be clearly seen in the zoom in Fig. 7.

The relative amplitude of the frequency components of the voltage obtained with the HB calculations (where the amplitudes obtained with time stepping serve as reference) is shown as a function of the spectrum (HB 1 to HB 13) in Fig. 8. Notice that the error of the fundamental $f$ component diminishes from only 1.2% with HB1 to less than 0.04% with HB 13. HB 13 produces an equally good precision for the $3f$ and $5f$ components (error of 0.3% and 0.05% respectively). The minimum error of the $7f$ and $9f$ is about 5%.

The calculated waveforms of the radial induction in two points in a stator tooth are shown in Figs. 9. It concerns the stator tooth that is aligned with the magnet in Fig. 2 and following, and two points on its axis of symmetry, one close to the airgap (at $r = 26.1$ mm) and the other further from the airgap (at $r = 30$ mm). Again an excellent agreement of the time stepping results and the HB results can be observed.

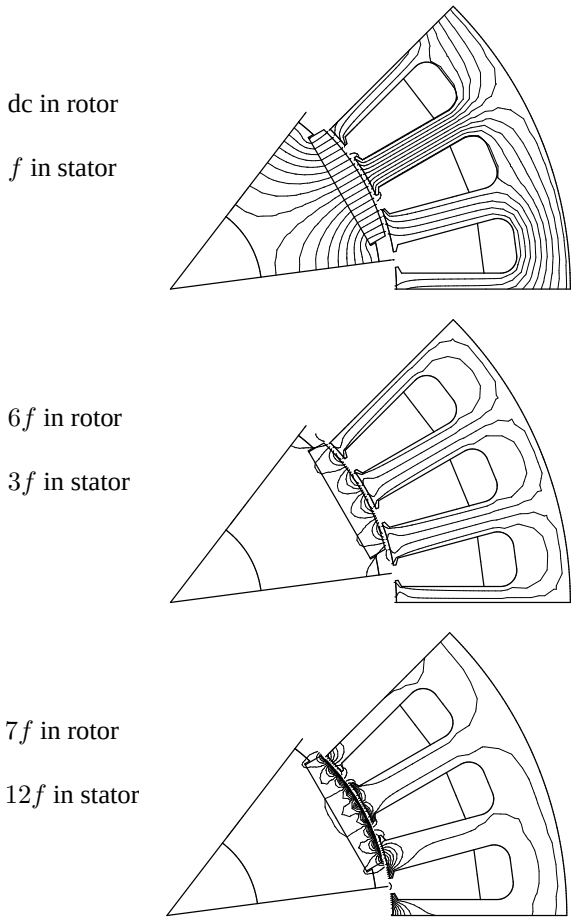


Fig. 6. Harmonic components of the flux pattern in the rotor and the stator

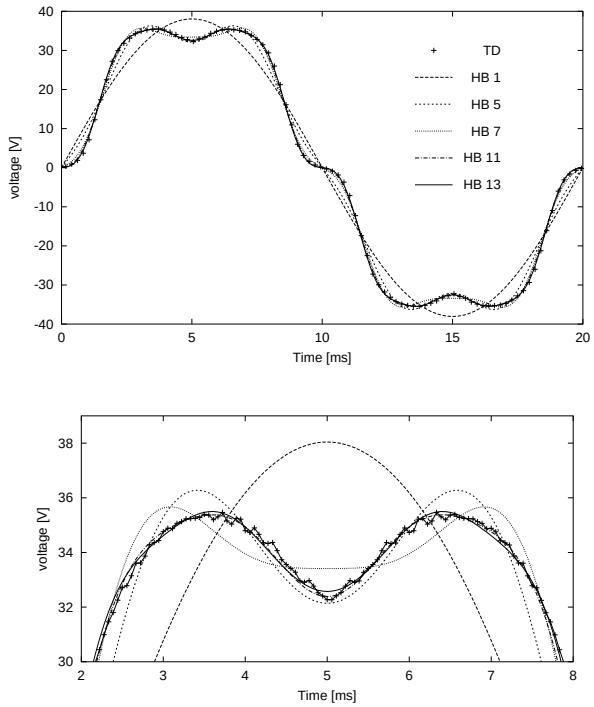


Fig. 7. Waveform of noload phase voltage obtained with time stepping and with the five HB calculations (same legend for zoom below)

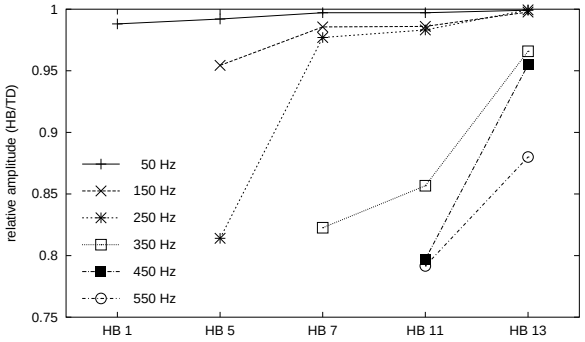


Fig. 8. Relative amplitude of the frequency components $f = 50\,\text{Hz}$ to $11f = 550\,\text{Hz}$ of the voltage obtained with the HB calculations (where the amplitudes obtained with time stepping serve as reference) as a function of the spectrum (HB 1 to HB 13)

In Fig. 10, the radial induction waveforms in two points in the rotor are depicted. The two points are situated on the symmetry axis of the permanent magnet, one close to the airgap (at $r = 25\,\text{mm}$) and the other further from the airgap (at $r = 20\,\text{mm}$). As the harmonics are multiples of six, only one sixth of a fundamental period, $[0, T/6]$, is shown.

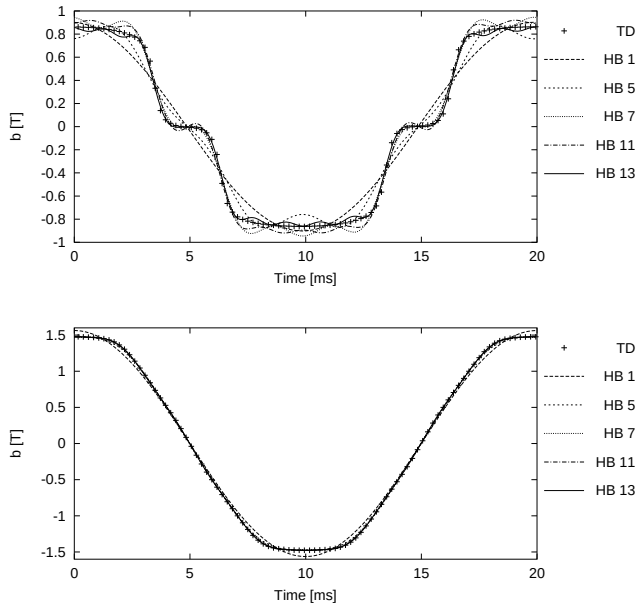


Fig. 9. Time-stepping and HB waveforms of the radial induction in two points in a stator tooth: a point close to the airgap (up) and a point further from the airgap (below)

### *D. Calculation times*

All calculation have been carried out on a Pentium III 750 MHz. The approximate calculation times supplied hereafter should give an indication of computational efficiency of the HB approach with regard to the stepping approach.

The time stepping simulation (one period, 360 steps, in average 3 NR iterations per time step) has taken 360 s. The HB calculations HB 1, HB 5, HB 7, HB 11 and HB 13 have taken 20 s, 67 s, 153 s, 310 s and 590 s respectively. The number of NR iterations was 7, 5, 4, 4 and 4 respectively. For HB 5 to HB 13, the previous solution (i.e. HB 1 to HB

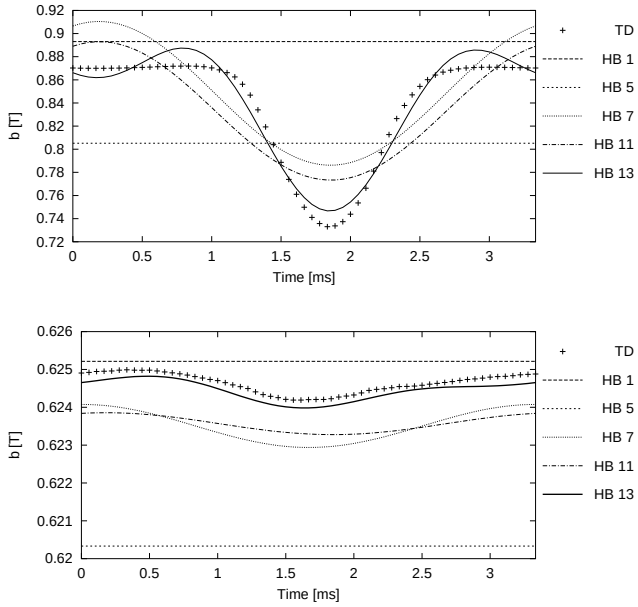


Fig. 10. Time-stepping and HB waveforms of the radial induction in two points in the permanent magnet: a point close to the airgap (up) and a point far from the airgap (below)

11) has been used as initial solution for the NR iterative process. Without this initialisation, the number of NR iterations was either 7 or 8.

If only the fundamental component $f$ and some lower order harmonics ($3f$, $5f$) are of interest, the HB approach is certainly more efficient than the time domain approach.

## 4. Conclusions

An original method to take into account movement in the 2D harmonic balance finite element modelling of electrical machines has been presented. The harmonic balance system of algebraic equations has been straightforwardly derived by applying the Galerkin approach to both the space and the time discretisation. The method can be easily implemented as it only requires some elementary manipulations of the moving band stiffness matrix. Magnetic saturation and electrical circuit coupling are easily included in the HBFE analysis.

The proposed method has been successfully applied to a permanent-magnet machine. The HB waveforms of the noload voltage converge well to the one obtained with time stepping. The computational cost of the HB calculations is favourable provided the number of considered frequency is not too big. Further research will involve the load simulation of the permanent-magnet machine.

## Acknowledgement

The research was carried out in the frame of the Inter-University Attraction Poles for fundamental research funded by the Belgian State. L. Vandevelde is Postdoctoral Fellow of the Fund for Scientific Research - Flanders (F.W.O.–Vlaanderen). P. Dular is a Research Associate with the Belgian Fund for Scientific Research (F.N.R.S.).

## References

[1] S. Yamada and K. Bessho, "Harmonic field calculation by the combination of finite element analysis and harmonic balance method", *IEEE Trans. Magn.*, vol. 24, pp. 2588–2590, Nov. 1988.

[2] J. Lu, S. Yamada and K. Bessho, "Harmonic balance finite element method taking account of external circuits and motion", *IEEE Trans. Magn.*, vol. 27, pp. 4024–4027, Sept. 1991.

[3] J. Gyselinck, P. Dular, C. Geuzaine and W. Legros, "Harmonic balance finite element modelling of electromagnetic devices: a novel approach", *IEEE Trans. Magn.*, vol. 38, pp. 521–524, March 2002.

[4] J. Gyselinck, C. Geuzaine, P. Dular and W. Legros, "Multiharmonic modelling of motional magnetic field problems using a hybrid finite element – boundary element discretisation", Proceedings of the Second International Conference on Advanced Computational Methods in Engineering (ACOMEN), May 28–31, 2002.

[5] A. Yahiaoui and F. Bouillault, "Saturation effect on the electromagnetic behaviour of an induction machine", *IEEE Trans. Magn.*, vol. 31, no. 3, pp. 2036–2039, May 1985.

[6] J. Luomi, A. Niemenmaa and A. Arkkio, "On the use of effective reluctivities in magnetic field analysis of induction motors fed from sinusoidal voltage source", Proceedings of the International Conference on Electrical Machines, München, Germany, Sept. 8–10, pp. 706–709, 1986.

[7] H. De Gersem and K. Hameyer, "Air-Gap flux splitting for the time-harmonic finite-element simulation of single-phase induction machines", *IEEE Trans. on Magn.*, vol. 38, no. 2, pp. 1221–1224, March 2002.

[8] N. Ida and J. P. A. Bastos, *Electromagnetics and calculation of fields*, Springer-Verlag, New York, 1992.

[9] P. Lombard and G. Meunier, "A general method for electric and magnetic coupled problem in 2D and magnetodynamic domain", *IEEE Trans. Magn.*, vol. 28, pp. 1291–1294, March 1992.

[10] J. Gyselinck, P. Dular, C. Geuzaine, and W. Legros, "Two-dimensional harmonic balance finite element modelling of electromagnetic devices coupled to nonlinear circuits", to be presented at the *XVII Symposium Electromagnetic Phenomena in nonlinear Circuits (EPNC)*, Leuven, Belgium, July 1-3, 2002.

[11] Y. Saad, *Iterative Methods for Sparse Linear Systems*, 1996. PWS Publishing Company.

[12] *SPARSKIT: a basic tool-kit for sparse matrix computations*, `http://www.cs.umn.edu/Research/arpa/SPARSKIT/sparskit.html`.

[13] A. M. Oliveira, P. Kuo-Peng, N. Sadowski, M. S. Andrade, and J. P. A. Bastos, "A non-a priori approach to analyze electrical machines modeled by FEM connected to static converters", *IEEE Trans. Magn.*, vol. 38, pp. 933–936, March 2002.